Electron density modulation in a pulsed dual-frequency (2/13.56 MHz) dual-antenna inductively coupled plasma discharge

Nishant SirseAnurag MishraGeun Y. YeomAlbert R. Ellingboe

Electron density modulation in a pulsed dual-frequency (2/13.56 MHz) dual-antenna inductively coupled plasma discharge

Nishant Sirse[a)]
Plasma Research Laboratory, School of Physical Sciences, Dublin City University, Dublin 9, Ireland

Anurag Mishra
Department of Advanced Materials Science and Engineering, Sungkyunkwan University, Suwon, Gyeonggi-do 440-746, South Korea

Geun Y. Yeom
Department of Advanced Materials Science and Engineering, Sungkyunkwan University, Suwon, Gyeonggi-do 440-746, South Korea and SKKU Advanced Institute of Nanotechnology (SAINT), Sungkyunkwan University, Suwon, Gyeunggi-do 440-746, South Korea

Albert R. Ellingboe
Plasma Research Laboratory, School of Physical Sciences, Dublin City University, Dublin 9, Ireland and Department of Advanced Materials Science and Engineering, Sungkyunkwan University, Suwon, Gyeonggi-do 440-746, South Korea

The electron density, n_e, modulation is measured experimentally using a resonance hairpin probe in a pulsed, dual-frequency (2/13.56 MHz), dual-antenna, inductively coupled plasma discharge produced in argon-C_4F_8 (90–10) gas mixtures. The 2 MHz power is pulsed at a frequency of 1 kHz, whereas 13.56 MHz power is applied in continuous wave mode. The discharge is operated at a range of conditions covering 3–50 mTorr, 100–600 W 13.56 MHz power level, 300–600 W 2 MHz peak power level, and duty ratio of 10%–90%. The experimental results reveal that the quasisteady state n_e is greatly affected by the 2 MHz power levels and slightly affected by 13.56 MHz power levels. It is observed that the electron density increases by a factor of 2–2.5 on increasing 2 MHz power level from 300 to 600 W, whereas n_e increases by only ~20% for 13.56 MHz power levels of 100–600 W. The rise time and decay time constant of n_e monotonically decrease with an increase in either 2 or 13.56 MHz power level. This effect is stronger at low values of 2 MHz power level. For all the operating conditions, it is observed that the n_e overshoots at the beginning of the on-phase before relaxing to a quasisteady state value. The relative overshoot density (in percent) depends on 2 and 13.56 MHz power levels. On increasing gas pressure, the n_e at first increases, reaching to a maximum value, and then decreases with a further increase in gas pressure. The decay time constant of n_e increases monotonically with pressure, increasing rapidly up to 10 mTorr gas pressure and at a slower rate of rise to 50 mTorr. At a fixed 2/13.56 MHz power level and 10 mTorr gas pressure, the quasisteady state n_e shows maximum for 30%–40% duty ratio and decreases with a further increase in duty ratio. © 2016 American Vacuum Society.
[http://dx.doi.org/10.1116/1.4959844]

I. INTRODUCTION

Low pressure nonequilibrium plasmas have found widespread applications in semiconductor processing technology. In particular, capacitive (CCPs) and inductively (ICPs) coupled radio frequency plasma discharges are widely investigated and used in the microelectronic industries for manufacturing integrated circuits.[1–6] Typically, CCPs operate in the pressure range of 1 mTorr–1 Torr and produce excellent plasma uniformity over the substrate, but are limited to the plasma density up to the order of 10^{10} cm^{-3}. Furthermore, the total independent control of the ion flux and the ion energy is not possible in a CCP even with the multiple frequency excitations.[6–8] Very high frequency (VHF) CCP discharges are proposed to achieve high plasma density (typically of the order of 10^{11} cm^{-3}) at reduced ion bombardment energies,[9–13] however

suffered major nonuniformity issues when the excitation wavelength becomes comparable to the reactor diameter and/or the skin-depth approaches the electrode gap.[14,15] To suppress this problem, VHF CCP discharges excited by segmented electrode are proposed and researched.[16–19] On the other hand, ICP discharges can overcome these limitations to some extent, i.e., the higher plasma density (up to 10^{11}–10^{12} cm^{-3}) is maintained at a very low pressure (<10 mTorr), and fully independent control of the ion bombardment energy is possible using a separate bias onto the substrate.[20] However, controllability of plasma uniformity over a large area remains the major challenge.

Multiple antenna ICPs are proposed and designed in order to scale up the conventional single frequency ICPs for large-area device fabrication.[21–23] The rationale of multiple-antenna ICPs is to increase the coil area by keeping the coil inductance low enough to enable efficient RF matching and uniform plasma over the large-area substrate size. Based on

a)Electronic mail: nishant.sirse@dcu.ie

this concept, a dual-frequency (2/13.56 MHz), dual-antenna ICP (12 turn inner coil powered by 2 MHz and three turn outer coil powered by 13.56 MHz) has been designed. The system has shown not only a more uniform plasma distribution over a large-area substrate (wafer size of 450 mm in diameter)[23] but also enhanced plasma density and reduction in the electron temperature when compared to the single-antenna, single-frequency plasma excitation.[24] The role of outer 13.56 MHz powered coil also serves to control the radial boundaries of the plasma. It has been demonstrated that the plasma parameters, including electron energy distribution function, are significantly modulated by choosing different combination of 2 and 13.56 MHz power levels.[25] Futhermore, the 2/13.56 MHz power combination has shown tailoring of ion energy distribution function to better control the etching and deposition profile.[26]

Pulsing a discharge system is an another efficient way of modulating the plasma parameters and has been utilized in the plasma etching applications.[27,28] In contrast to continuous wave (CW) plasmas, pulsed plasma produces a higher plasma density for the same average power.[29] In the pulsed plasma system, the power is actively deposited for only a fraction of time depending on the duty ratio/pulse repetition frequency. This offers the possibility of working with low ion energy regimes and less dissociated plasma. Both of these features of pulsed plasma extenuate the plasma induced damage to the substrate. Pulsing effectively controls the composition of reactive species in the discharge system and thus provides a highly selective etch profile when applied to plasma etching.[30] In the dual-frequency, dual-antenna plasma system described above, both 2 and 13.56 MHz pulsing have been demonstrated.[31–33] In Argon discharge, pulsing 2 MHz and different combination of 2/13.56 MHz power levels has shown significant modulation in the plasma potential during the pulse-off phase.[31] From an estimate of electron temperature from plasma potential and floating potential measured by floating emmisive probe, it was found that the effect of increasing 2 MHz power level is to lower the electron temperature; however, increasing 13.56 MHz power increases the electron temperature.[31] Langmuir probe study under the same set-up and similar discharge conditions has predicted a slow rise in the electron density during the 2 MHz pulse-on phase in order to reach to a quasisteady state value.[32] The plasma potential has shown a similar trend as measured by the emissive probe over a course of one pulse period, whereas the electron temperature confirmed the emissive probe measurements only when the density reached to a quasisteady state value and in the early afterglow. During the pulse-on phase and late afterglow, the electron temperature predicted an opposite trend, i.e., an increase in electron temperature with an increase in 2 MHz power level and attributed to capacitive to inductive transition. More recently, the effect of pulsing 2 and 13.56 MHz on SiO_2 etching over amorphous carbon layer has been investigated[33] in the $Ar-C_4F_8$ gas mixture. The results showed increased etch selectivity due to the decrease in the average electron temperature and change in the gas decomposition. The system has also shown improved plasma

uniformity at reduced duty ratio when compared to CW plasma which is highly desirable for large-area processing.

In this paper, we present the effect of pulsing on the temporal evolution of electron density in a pulsed, dual-frequency (2/13.56 MHz), dual-antenna, inductively coupled plasma discharge in $Ar-C_4F_8$ (90–10) gas mixture. Measurements in Ar discharge was previously reported[21,31] for inferring fundamental characteristics of this dual-frequency, dual-antenna ICP system. Here, we extended our study to the pulsed electronegative $Ar-C_4F_8$, which was recently used[33] in the same set-up to investigate the etch characteristics of SiO_2 over the amorphous carbon layer. The effect of low and high frequency power levels, gas pressure, and duty ratio is systemically investigated in this article.

II. EXPERIMENT

A. Description of the apparatus

A schematic of the two-frequency dual-antenna inductively coupled plasma discharge is shown in Fig. 1. The discharge is produced in a cylindrical, anodized-aluminum chamber with an internal diameter of 630 mm and height 60 mm by using two planar concentric spiral coils with 12 and three turns, respectively. The coils are separated from the plasma via a 35 mm thick dielectric (quartz) window. The inner coil is powered at 2 MHz (NOVA-50A, ENI), and the outer coil is powered at 13.56 MHz (CX-5000S, COMDEL) with two separate matching networks. The output of the 2 MHz power generator is pulsed using a pulsing unit with an ability to change the pulsing frequency and duty cycle. During pulsing, both 2 and 13.56 MHz power systems are first tuned in the CW mode using their individual matching networks, and thereafter, 2 MHz is pulsed for the fixed capacitors values. The reflected power in the pulse mode was less than 5% of the total input power. The discharge is produced in the $Ar-C_4F_8$ (90–10) gas mixture. The individual gas flow rate is controlled by using two separate mass flow controllers (MFC1 and MFC2) as shown in Fig. 1. A multi-hole shower ring is located inside the plasma chamber for a distributed gas flow. The gas pressure inside the chamber is regulated by a mass flow controller (2900 series, Tylan) together with an adaptive pressure controller (PM-7, VAT) for the gate valve control above a turbomolecular pump backed by a dry pump.

B. Diagnostic technique

The time resolved electron density is measured using a resonance hairpin probe. The hairpin probe employed in this study is a fully floating resonance hairpin probe,[7,34,35] i.e., the probe tip is electrically isolated from the coupling loop so that it can follow the plasma potential oscillation. In this type of probe design, the microwave power is coupled inductively to the hairpin structure. To maximize the coupling between the hairpin structure and the induction loop, a two turn helical induction loop is constructed at the extreme end of the high temperature 50 Ω coaxial cable. The high temperature coaxial cable and the coupling loop are enclosed in a one end closed ceramic tube having a groove at the extreme
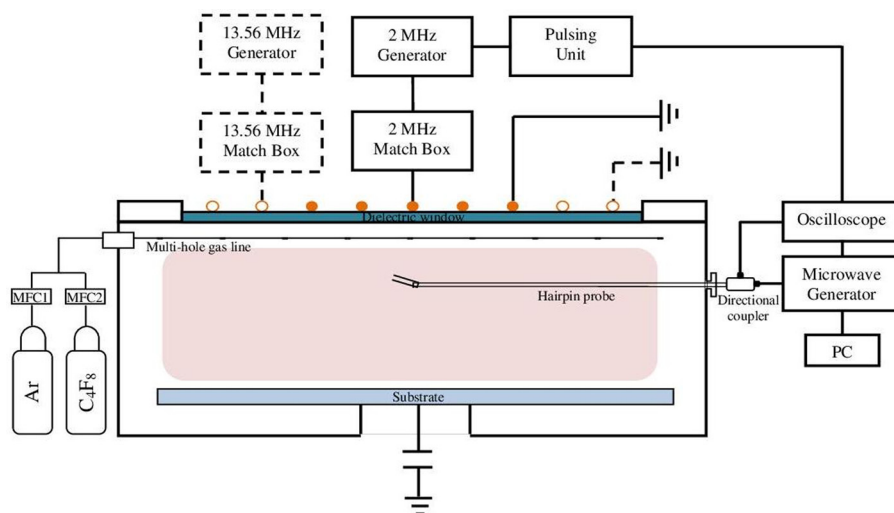
FIG. 1. (Color online) Schematic of dual frequency ICP system along with the hairpin probe and its data acquisition system.

end to support the probe tip. The probe tip is made from a 0.25 mm diameter gold coated tungsten wire. The length and width of the probe tip are 3 cm and 4 mm, respectively, resulting in a measured vacuum resonance of 2.3 GHz. The probe resonance frequency is obtained experimentally by scanning the microwave frequency from 2 to 4 GHz in vacuum. At resonance, microwave power couples into the hairpin structure and the amplitude of the reflected signal drops to zero which gives a sharp resonance peak (20–30 MHz FWHM). The probe is positioned at the center of the discharge (r = 0 cm) and ∼2 cm below from the dielectric window.

The hairpin structure is excited by driving an AC to the induction loop using a Hewlett Packard HP8350 microwave generator with a sweep range from 10 MHz to 8 GHz. The reflected signal from the coupling loop is measured using a Schottky diode and recorded on the oscilloscope (Tektronix TDS3034B 300 MHz). At resonance, microwave power couples into the hairpin structure and the magnitude of the reflected signal drops sharply. This allows a precise measurement of the resonance frequency. In a collision-less non-magnetized plasma, the electron density is described by the formula[36]

$$n_e = \frac{f_r^2 - f_0^2}{0.81},\qquad(1)$$

where both f_r and f_0 are the plasma resonance and vacuum resonance frequency, respectively, measured in GHz and n_e is in units of $10^{10}\,\text{cm}^{-3}$. In the above formula, the correction due to sheath is neglected.

The technique for measuring time resolved electron density using a resonance hairpin probe is described previously and applied in several pulse plasma systems.[35,37–39] Briefly, to obtain the resonance signal in the time resolved mode, a single frequency output from the microwave generator is generated and applied to the hairpin structure. The reflected signal is recorded as a function of time within the pulse. If the probe is in resonance at any point in time during the

pulse, the probe displays minimum in the reflected signal. Assuming that the electron density dynamic is repeated at each trigger pulse, then it is possible to tune the microwave generator to a next higher frequency which will allow the probe to resonate at a later time for different densities. The process can be repeated to obtain a spectrum of probe resonance frequencies as a function of time and hence the electron density versus time by using Eq. (1). In this experiment, the frequency output of the microwave generator is controlled by a LABVIEW program (developed at DCU, Ireland) along with the synchronous recording of the reflected signal from the oscilloscope. The output frequency is scanned from 2 to 5 GHz in the step size of 2 MHz which is defined by the number of steps given by $n = (f_f - f_i)/\Delta f$, where f_i and f_f are start and stop frequency, respectively, and Δf is the step size. In order to improve the signal to noise ratio, the background signal (i.e., without plasma) at each frequency is subtracted from the plasma signal.[7,34]

III. RESULTS AND DISCUSSION

A. Effect of rf power levels

Figures 2(a)–2(d) show the temporal evolution of electron density over one pulse period measured for different 2 and 13.56 MHz power levels at a fixed gas pressure of 10 mTorr in Ar-C$_4$F$_8$ (90–10) gas mixture. Power of 2 MHz is pulsed at a frequency of 1 kHz, 50% duty ratio, whereas 13.56 MHz is applied in the CW mode. As shown in Fig. 2, the rf-on pulse triggers the data collection at t = 0, and the electron density modulates synchronously with the 2 MHz pulse. It is observed that the electron density reaches a quasisteady state value in the longer on-phase and falls during the off-phase of the plasma. As displayed in Figs. 2(a)–2(d), the quasisteady state electron density is greatly affected by the 2 MHz power levels; however, it is slightly affected by 13.56 MHz power levels. It is observed that the quasisteady state electron density increases by a factor of ∼2–2.5 on increasing the 2 MHz power level from 300 to 600 W for different 13.56 MHz power levels. However, for a fixed 2 MHz power level, i.e.,
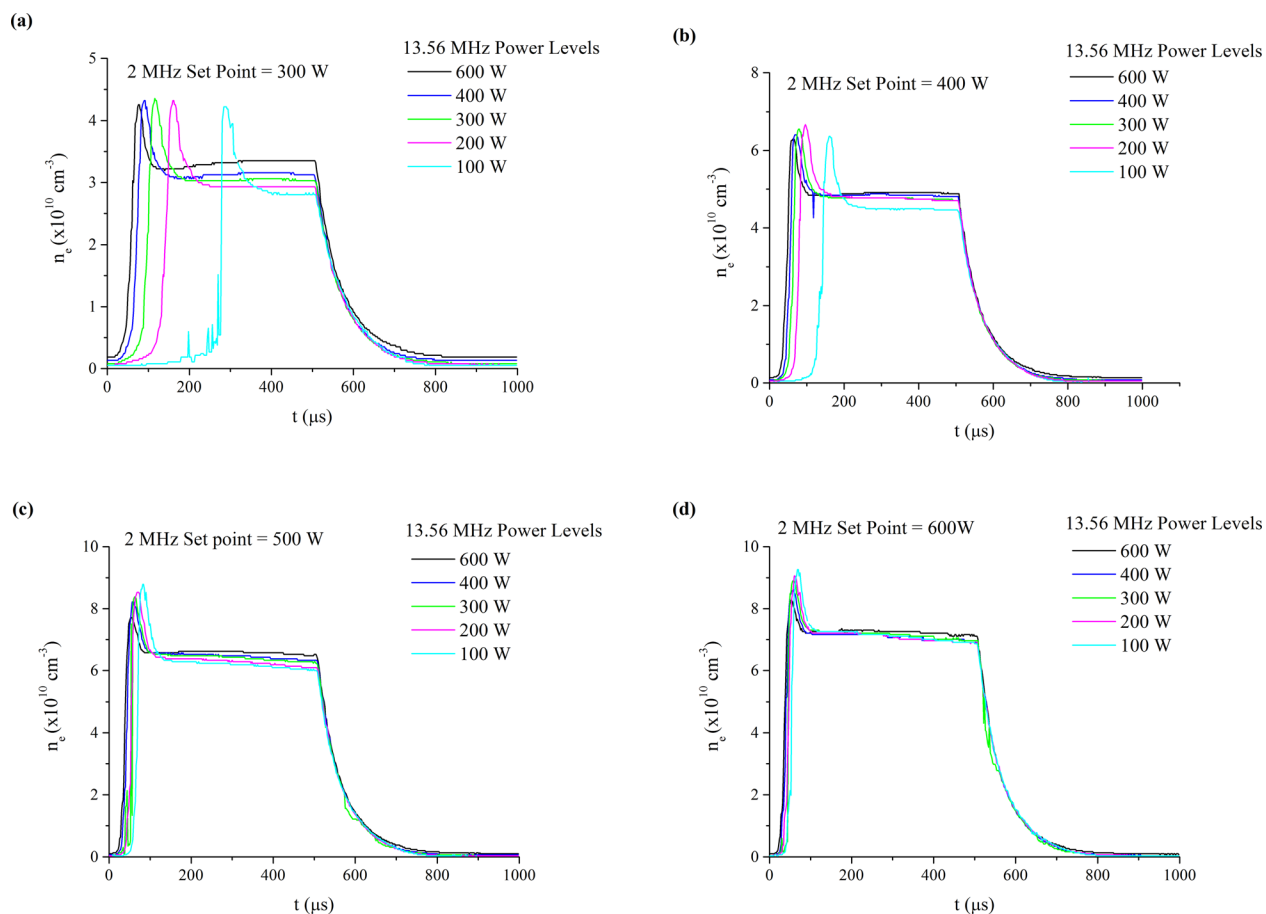
FIG. 2. (Color online) Temporal evolution of electron density for different 13.56 MHz power levels at a fixed gas pressure of 10 mTorr. Power levels of 2 MHz are (a) 300 W, (b) 400 W, (c) 500 W, and (d) 600 W. Two megahertz is pulsed at a frequency of 1 kHz, and 13.56 MHz is applied in the CW mode.

from 300 to 600 W, an increase in the electron density with an increase in 13.56 MHz power level (100–600 W) is less than 20%. This is summarized in Fig. 3.

The increase in the quasisteady state electron density due to the increase in rf power levels is mainly attributed to the increase in power dissipation into the plasma volume. At a fixed gas pressure, power absorbed by plasma electrons from the driven antenna mostly dissipates into the electron collisions with other species and therefore produces a higher electron density by either single or multistep ionization process. As displayed in Fig. 3, the effect of 2 MHz power levels on the steady state electron density is higher when compared to 13.56 MHz. One of the possible reason for this discrepancy is the location of the probe where the measurement is performed with respect to the plasma region heated by mostly 13.56 MHz. Since the probe is located at the centre of the discharge, i.e., far from the coil excited at 13.56 MHz, therefore its effect would be smaller on the quasisteady state electron density. As discussed before, the rationale of outer antenna excited at 13.56 MHz is to control the radial boundaries. Another possible reason is the higher power absorption at low (2 MHz) driving frequency. It is well known that ohmic heating in the plasma volume is proportional to the electric field strength which is inversely proportional to the driving frequency;[22] thus, a higher electric field is expected at 2 MHz driving frequency compared to 13.56 MHz, which

produces a higher plasma density. Previously, in Ar discharge and in the same set-up, it was shown that a higher plasma density is produced by two antennae energized by 2 and 13.56 MHz when compared to a single coil energized by 13.56 MHz for the same total input power.[24]

For all the operating conditions studied here, it is noticed that the plasma density overshoots in the beginning of on-phase before relaxing to a quasisteady state value. These
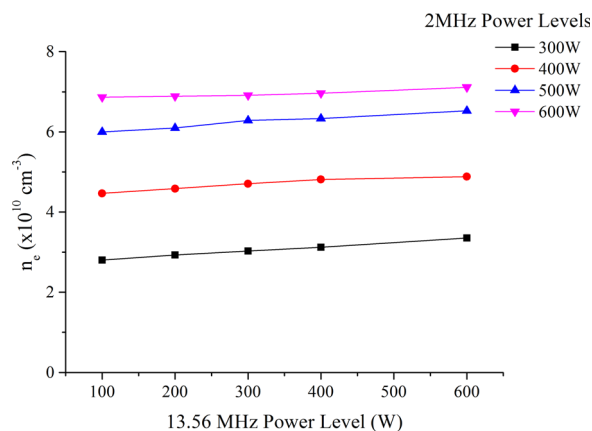

FIG. 3. (Color online) Quasisteady state electron density for different 2 and 13.56 MHz power levels at a fixed gas pressure of 10 mTorr. Two megahertz is pulsed at a frequency of 1 kHz, and 13.56 MHz is applied in the CW mode.

results are in contradiction with the previously published work in Ar plasma in the same setup.[32] In Ar discharge, the plasma density overshoots were observed at the beginning of early afterglow, which was attributed to the thin to thick sheath transition limiting the probe theory. In this case, the hairpin probe is used to measure the electron density which is a fully floating probe, i.e., not drawing any current from the plasma and therefore independent of the above mentioned effect. The relative overshoot $[100 \times (n_{ep} - n_{eb})/n_{eb}]$, where n_{ep} and n_{eb} represents peak and background densities, respectively, and the rise time of electron density are plotted in Figs. 4 and 5, respectively. The rise time of the electron density is measured from the pulse on-phase (i.e., from $0\,\mu$s) to the time at which the electron density reaches its peak value. It is observed that both the electron density overshoot and the rise time of the electron density are significantly affected by the 13.56 and 2 MHz power levels. As shown in Fig. 4, the electron density overshoot decreases (almost linearly) with an increase in 2 and 13.56 MHz power levels. At 300 W 2 MHz peak power, the overshoot in the electron density drops from 50% (at 100 W 13.56 MHz power level) to 25% (at 600 W 13.56 MHz power level). Similar to the density overshoot, the rise time of the electron density decreases with an increase in the 2 and 13.56 MHz power levels. However, the effect of the 13.56 MHz power level on the rise time of electron density is higher at low values of 2 MHz peak power. At 300 W 2 MHz peak power level, it is noticed that the rise time of the electron density decreases by ~73% on increasing 13.56 MHz power level from 100 to 600 W, whereas at 600 W 2 MHz peak power, the rise time decreases by ~20%. One possible explanation for the electron density overshoot is low plasma conductivity at the beginning of plasma on-phase. This is due to the low electron density at the end of the plasma off-phase. The low n_e causes the electric field strength to increase at the beginning of on-phase and therefore produces a higher electric field and high plasma ionization rate. As shown in Fig. 4, the overshoot electron density decreases with an increase in the 13.56 MHz power, which is mainly attributed to the rise in the plasma conductivity at the beginning of the on-phase with

Fig. 5. (Color online) Electron density rise time vs 2 and 13.56 MHz power levels at a fixed gas pressure of 10 mTorr. Two megahertz is pulsed at a frequency of 1 kHz, and 13.56 MHz is applied in the CW mode.

greater 13.56 MHz power. During the pulse off-phase, the plasma is sustained by 13.56 MHz power level. With 13.56 MHz turned-on, the plasma electrons remain heated in the 2 MHz pulse off-phase, albeit with lower ionization efficiency. The ionization rate depends on the applied rf power level, i.e., the plasma maintains a higher electron density at high 13.56 MHz power in comparison to its low power [shown in Fig. 2(a)]. Also, in a previous experimental study, it was shown that the electron temperature in the 2 MHz pulsed off phase increases with an increase in 13.56 MHz power level.[31] Similar results were obtained by Malyshev and Donnelly[40] in a pulsed inductively coupled chlorine plasma with a continuous substrate bias. In this study, it was shown that the electrons are significantly heated in the long off-phase with the substrate bias on in comparison to no substrate bias. Thus, a decrease in the overshoot density is mainly attributed to the increased plasma conductivity at the beginning of the on-phase due to the increase in the electron density/thermal velocity. On increasing 2 MHz power level, the electron density is higher at the beginning of the decay phase, and therefore, it has a relatively higher value at the end of the pulse off-phase with a constant 13.56 MHz power level, which in turn increases the plasma conductivity. Similar to the overshoot densities, the decreasing rise time of the electron density is mainly attributed to the plasma conductivity at the beginning of the on-phase. As 13.56 MHz power level increases, the 2 MHz pulse power sees higher plasma conductivity, and therefore, in a shorter time, the electron avalanche is achieved followed by the steady state plasma in longer on-time.

As shown in Fig. 2, in the afterglow plasma, the electron density decays as a function of time and reaches to its lowest values depending on the 13.56 MHz power level. The characteristic decay of electron density in the afterglow plasma can be described by the global model of pulsed plasma.[41] According to the global model of the pulsed plasma, the temporal evolution of the electron density in the afterglow plasma can be described by the equation $(1/n_e)(dn_e/dt) \approx \nu_{iz} - \nu_{loss}$, where ν_{iz} and ν_{loss} are the time dependent ionization rate and the characteristic particle loss rate, respectively. Assuming $\nu_{iz} \ll \nu_{loss}$ and the weak dependence of ν_{loss} ($\nu_{loss} \propto T_e^{1/2}$) on
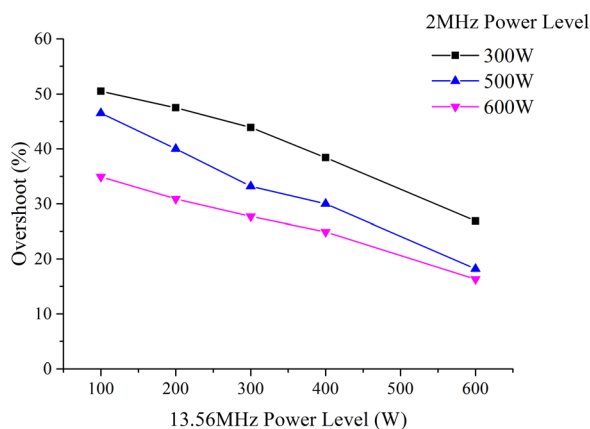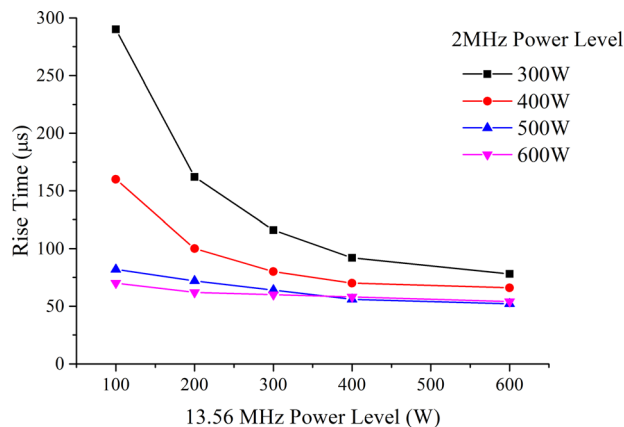

Fig. 4. (Color online) Electron density overshoot for different 2 and 13.56 MHz power levels at a fixed gas pressure of 10 mTorr. Two megahertz is pulsed at a frequency of 1 kHz, and 13.56 MHz is applied in the CW mode.

electron temperature, i.e., $\nu_{\text{loss}} = $ constant, the above equation shows simple exponential decay of the electron density, $n_e(t) = n_0 e^{-t/\tau}$, where n_0 is the initial steady state value and τ is the characteristic decay time of the electron density. Our data support a single exponential decay (see Fig. 2) with the decay time constant plotted in Fig. 6 for different values of 2 and 13.56 MHz power levels. Note that the decay phase is actually a transition between two self-consistent plasma density values; a high n_e when 2 MHz is on and a low n_e with 2 MHz off. Because 13.56 MHz power level is always on, the electron temperature does not collapse but is kept somewhat high due to heat flow from 13.56 MHz heated regions to the central volume. It is observed that the decay time constant decreases with an increase in both 2 and 13.56 MHz power levels. Similar to the density rise time, the effect of the 13.56 MHz power level on the decay time constant is higher at low values of 2 MHz peak power. At 300 W of 2 MHz peak power, the decay time constant decreases by ~12% when 13.56 MHz power level is increased from 100 to 600 W, whereas at 600 W, 2 MHz peak power, the same decreases by ~5%. This effect may be attributed to the dependence of the loss rate on the electron temperature. In the absence of 13.56 and 2 MHz, the electrons quickly cool down and the loss rate decreases.[42] However, with 13.56 MHz powers remaining on during the 2 MHz off-cycle electrons are heated significantly, and therefore, the loss rate of the electrons remains high during the off-phase. In the previous experimental studies done under the same setup and similar operating conditions in Ar discharge, it was shown that the electron temperature in the afterglow plasma is affected by both 2 and 13.56 MHz power levels.[31] At a constant 2 MHz power level on increasing 13.56 MHz power level, the electron temperature increases, and therefore, the electron loss rate increases. Similar results have been observed in a pulsed two-frequency capacitively coupled plasma discharge.[39]

B. Effect of gas pressure

Figure 7 shows the measured plasma density evolution over a course of one pulse period for different gas pressures. During these measurements, 13.56 MHz is applied in the CW mode at a fixed power level of 600 W, and 2 MHz power

is pulsed at a frequency of 1 kHz with 50% duty cycle and 600 W peak power. Figure 8 plots the quasisteady state n_e (from the end of the on-cycle) versus pressure, which exhibits a moderate increase with pressure in the 3–10 mTorr range, then falling with a further increase in pressure. This behavior was seen previously in both steady/pulsed capacitive,[39,43] inductively coupled[44] radio frequency electronegative discharges and also predicted by the global model.[45] The dependence of the quasisteady state electron density on gas pressure could be explained on the basis of production and loss mechanism of electrons in the discharge. The main production mechanism is the ionization of neutral gas molecules. At a low gas pressure, the electrons are mainly lost through diffusion toward the chamber walls. Apart from the wall losses, electrons are also lost through volumetric processes, recombination of thermalized electron with molecular ions, and nondissociative attachment of thermalized electrons to molecules and radicals, for example. These play a significant role at high gas pressures. Furthermore, C_4F_8 is an electronegative gas and has a strong tendency to form negative ions.[46–48] These negative ions are predominately formed by the dissociative attachment process and thus produce an additional electron loss channel. The electron density dependence on the gas pressure is balanced by various production and loss mechanism. In the low pressure regime, i.e., up to 10 mTorr, the mean free path of electrons is greater than the discharge gap, and therefore, a high electron temperature is required to give sufficient ionization to maintain steady state condition of the plasma. As the gas pressure further increases, the mean free path of electrons decreases, the electron temperature decreases, and in turn this decreases the wall losses. The energy loss per electron–ion pair continues to increase with gas pressure due to enhanced collision rates. A competition between the wall losses and the energy loss per electron-ion pair might be responsible for the observed trend in the quasisteady state electron density at a high gas pressure. In addition to the wall losses, the volumetric losses continue to decrease the electron density at a high gas pressure; however, its contribution to the observed trend is vague
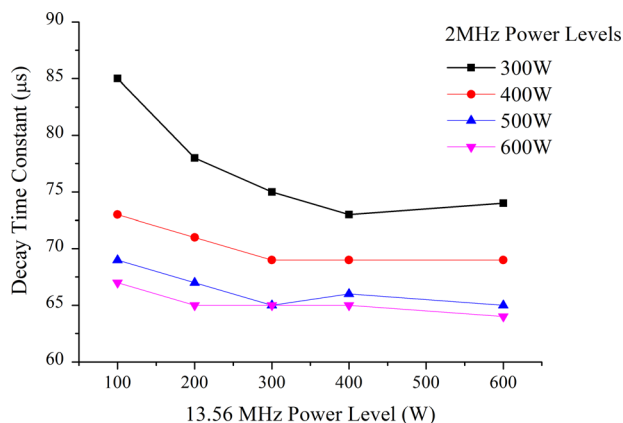

FIG. 6. (Color online) Decay time constant vs 2 and 13.56 MHz power levels at a fixed gas pressure of 10 mTorr. Two megahertz is pulsed at a frequency of 1 kHz, and 13.56 MHz is applied in the CW mode.
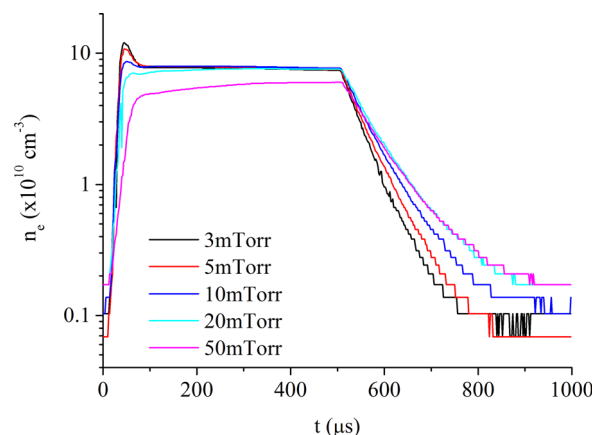

FIG. 7. (Color online) Temporal evolution of electron density as a function of gas pressure. Peak power level of 2 MHz is 600 W and pulsed at a frequency of 1 kHz with 50% duty ratio. Power level of 13.56 MHz is 600 W and applied in the CW mode.
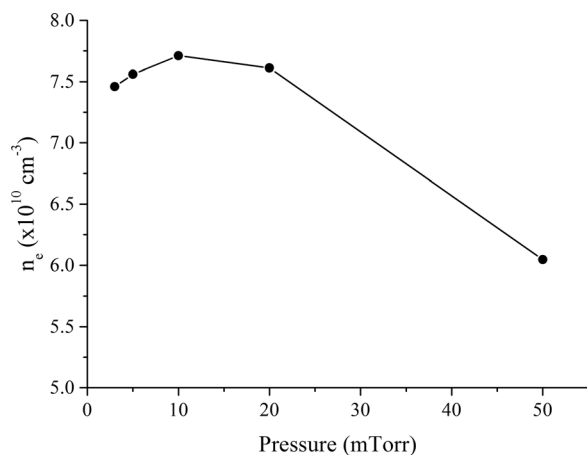
FIG. 8. Quasisteady state electron density as a function of gas pressures. Peak power level of 2 MHz is 600 W and pulsed at a frequency of 1 kHz with 50% duty ratio. Power level of 13.56 MHz is 600 W and applied in the CW mode.
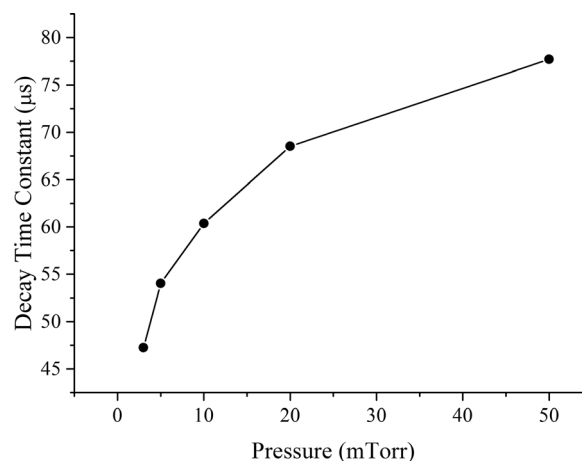

FIG. 9. Decay time constant of electron density as a function of gas pressures. Peak power level of 2 MHz is 600 W and pulsed at a frequency of 1 kHz with 50% duty ratio. Power level of 13.56 MHz is 600 W and applied in the CW mode.

and beyond the scope of this work. Another possible reason for the low electron density at a high gas pressure is that the plasma density localization is away from the center of the discharge in the inductively coupled plasma.[49] This effect is mainly due to localized gas heating in the vicinity of the coils caused by the electric field of the antenna. At a high gas pressure, the mean free path of the electron is small; thus, the high energy electrons are less distributed and therefore produce a high plasma density locally.

Figure 9 shows the decay time constant of the electron density as a function of gas pressure, which increases from ∼47 μs at a 3 mTorr gas pressure to ∼78 μs at 50 mTorr gas pressure. The growth of decay time constant is fast up to 10 mTorr gas pressure and then slows at higher gas pressures. An increase in the decay time constant with the rise in gas pressure can be attributed to a decrease in the electron temperature.[42] The electron temperature can be estimated by the decay time constant based on electron loss mechanism. In a low pressure plasma, the surface loss is by-far dominant loss mechanism, and the decay rate is described by the Bohm flux ($u_B = \sqrt{kT_e/M}$, where k is Boltzmann constant, T_e is electron temperature, and M is the mass of positive ions) to the surface. At a gas pressure of 3 mTorr, the measured n_e shows (Fig. 7) an approximately linear slope in the log-linear plot in the first 100 μs in the afterglow plasma with a decay time-constant of ∼47 μs. Assuming a negligible electron loss in the radial direction compared to the axial direction due to the much longer distance involved, an approximate 3 cm (half of the discharge gap) characteristic decay length corresponds to an electron temperature of 1.7 eV. The dominant positive ion species considered in the calculation are fluorocarbon ions with an atomic mass of 100 amu.[50] In contrast, at 50 mTorr gas pressure, the characteristic decay time constant of ∼78 μs equates to an electron temperature of ∼0.6 eV. These values are within a factor of 2 predicted by a simple global-model power-balance argument.[51] Therefore, in the pressure range of 3–50 mTorr, the electron temperature estimated by the decay time constant based on the surface losses as dominant loss mechanism is

decreased by ∼65%. Note that the volumetric electron losses at high gas pressure possibly play an important role in estimating the electron temperature from the decay time constant; however, it is beyond the scope of this work. Further possible reason for the slow increase in the density decay time constant at higher gas pressure is an electron generation process in the afterglow plasma. Due to electron generation, the electron loss rate decreases, and therefore, the electron density decay slows down. This is apparent from the electron density decay shown in Fig. 7 at 50 mTorr gas pressure. One of the possibilities of the electron generation in C_4F_8 plasma is the destruction of negative ions. In C_4F_8 plasma, the dominant negative ion is F^-,[46,48] and $C_4F^-_8$ is also present, which can easily autodetach due to large rate constant.[52] Thus, the electron generation by the associative collisional detachment of F^- according to the reaction $F^- + CF_x \rightarrow CF_{x+1} + e$ (where x = 1–3) possibly slows down the electron density decay in the late afterglow.

Furthermore, at low pressures, i.e., from 3 to 10 mTorr, an overshoot in the electron density overshoot at the beginning of on-phase is seen. This overshoot is diminished with a further increase in the gas pressure. This effect is mainly due to the high electron density at the beginning of the on-phase and therefore higher conductivity of the plasma. As shown in Fig. 7 and discussed earlier, the electron density wall loss decreases with an increase in the gas pressure, and therefore, the discharge contains more electrons at the end of 2 MHz pulse off-phase, which reduces the electric field in the plasma.

C. Effect of duty ratio

Figure 10 shows the effect of the duty ratio on the electron density evolution. The duty ratio is varied from 10% to 90% at a fixed gas pressure of 10 mTorr. The 2 MHz is pulsed at a frequency of 1 KHz with a power level of 600 W, and 13.56 MHz is applied in the CW mode with a power level of 600 W. As shown in Fig. 10, the n_e reaches a quasisteady state value for all the duty ratios above 20%. However, at 10% and 20% duty ratio, the on-time is not sufficient for

n_e to reach to a quasisteady state value. Figure 11 shows the corresponding peak n_e in the pulse on-phase. It is observed that the peak n_e first increases with an increase in the duty ratio, reaching to a maximum value, between 30% and 40%, and then decreases with a further increase in the duty ratio. Furthermore, the n_e overshoot at the beginning of on-phase is observed at 50% and 75% duty ratio and disappeared at 90% duty ratio.

An initial increase in the peak n_e with increasing duty ratio suggests that the plasma on-time is not sufficient to achieve quasisteady state. However, with a further increase in the duty ratio, the peak n_e is decreasing. This may be attributed to the decrease in neutrals/metastables species densities that generates electrons by ionization process or an increase in the loss rates of electrons. The decrease in the neutral gas density is possible due to significant gas heating.[53,54] As the duty ratio increases, the neutral gas molecules are heated for longer time periods which decreases the local gas density due to the depletion of gas molecules. A further possible reason for the electron density peak between 30% and 40% duty ratio is gas dissociation and recombination, which is responsible for losses and production mechanism for several other atomic/molecular species with different ionization potentials. Increasing plasma off time increases the recombination probability of the dissociated gases and also controls the dissociation of C_4F_8 gas molecules. The previous experimental study under the same setup and similar operating conditions has shown a maximum in the CF_2/F density ratio at 30% and 40% duty ratio.[33] Thus, the increasing electron density with the decreasing duty ratio may be attributed to lower gas dissociation plasma which produces fewer F atoms since the ionization potential of atomic F (17 eV) is higher in comparison to the CF_2 and C_4F_8 (~11 eV) gas molecules. The low fractional dissociation gas-mixture at a low duty ratio results in higher electron (and ion) density. These results are similar to the one reported by Hebner and Fleddermann,[55] in chlorine pulse-modulated inductively coupled plasma where the low duty ratio resulted in a high molecular chlorine (Cl_2, 11.48 eV)

FIG. 11. Maximum plasma density in the pulse on-phase vs various duty ratios at 10 mTorr gas pressure. Peak power level of 2 MHz is 600 W and pulsed at a frequency of 1 kHz. Power level of 13.56 MHz is 600 W and applied in the CW mode.

and high n_e, whereas the high duty ratio resulted in high atomic chlorine (Cl, 12.97 eV) and low n_e. However, these results are in contrast with the work published by Agarwal *et al.*[56] in Ar-Cl_2 based ICP discharge where both the source and bias power is pulsed in full synchronization with no phase lag. They attributed this to the enhanced dissociation of the feedstock gases due to the longer plasma on-time.

IV. SUMMARY AND CONCLUSION

In summary, we have investigated the electron density modulation in a pulsed dual-frequency (2/13.56 MHz) dual-antenna ICP discharge produced in Ar-C_4F_8 gas mixture using the resonance hairpin probe. It is observed that the quasisteady state electron density is significantly affected by the 2 MHz power levels; however, it is slightly affected by the 13.56 MHz power levels. An overshoot in the electron density is observed at the beginning of the on-phase. The relative electron density overshoot decreases monotonically with an increase in the 2 and 13.56 MHz power levels. Both the rise time and decay time constant of the electron density decreases with an increase in the 2 and 13.56 MHz power levels. On increasing the gas pressure, the quasisteady electron density at first increases up to 10 mTorr and thereafter decreases, whereas the decay time constant continues to increase with the gas pressure. The peak electron density in the on-phase is maximum for a duty ratio between 30% and 40%, which is attributed to the less dissociated plasma and decreases with a further increase in the duty ratio.
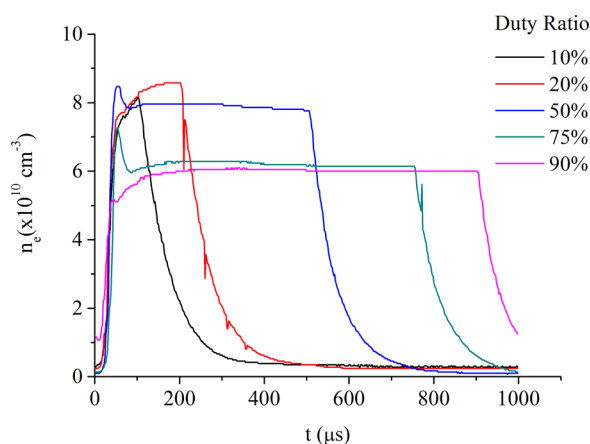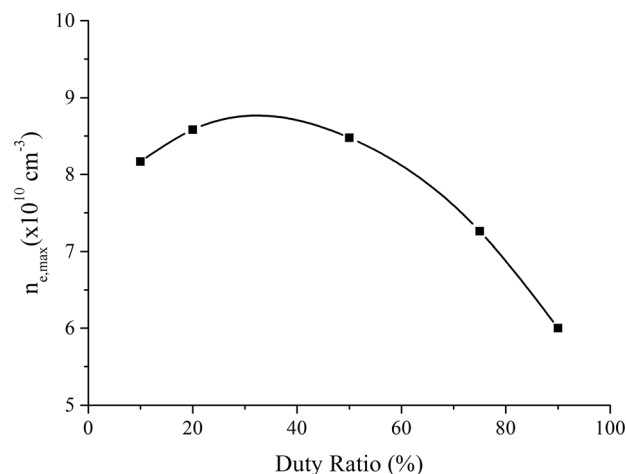
ACKNOWLEDGMENTS

FIG. 10. (Color online) Electron density evolution vs duty ratio at 10 mTorr gas pressure. Peak power level of 2 MHz is 600 W and pulsed at a frequency of 1 kHz. Power level of 13.56 MHz is 600 W and applied in the CW mode. Operating gas pressure is 10 mTorr.

[1]E. Kawamura, M. A. Lieberman, and A. J. Lichtenberg, Phys. Plasmas **13**, 053506 (2006).

[2]H. Goto, H. Lowe, and T. Ohmi, J. Vac. Sci. Technol., A **10**, 3048 (1992).

[3]J. Hopwood, Plasma Sources Sci. Technol. **1**, 109 (1992).

[4]P. L. G. Ventzek, R. J. Hoekstra, and M. J. Kushner, J. Vac. Sci. Technol., B **12**, 461 (1994).

[5]D. B. Graves, IEEE Trans. Plasma Science **22**, 31 (1994).

[6]P. C. Boyle, A. R. Ellingboe, and M. M. Turner, J. Phys. D: Appl. Phys. **37**, 697 (2004).

[7]S. K. Karkari and A. R. Ellingboe, Appl. Phys. Lett. **88**, 101501 (2006).

[8]T. Gans, J. Schulze, D. O'Connell, U. Czarnetzki, R. Faulkner, A. R. Ellingboe, and M. M. Turner, Appl. Phys. Lett. **89**, 261502 (2006).

[9]M. Surendra and D. B. Graves, Appl. Phys. Lett. **59**, 2091 (1991).

[10]V. Vahedi, C. K. Birdsall, M. A. Lieberman, G. DiPeso, and T. D. Rognlien, Phys. Fluids B **5**, 2719 (1993).

[11]M. J. Colgan, M. Meyyappan, and D. E. Murnick, Plasma Sources Sci. Technol. **3**, 181 (1994).

[12]W. Schwarzenbach, A. A. Howling, M. Fivaz, S. Brunner, and C. H. Hollenstein, J. Vac. Sci. Technol., A **14**, 132 (1996).

[13]T. Katajima, Y. Takeo, N. Nakano, and T. Makabe, J. Appl. Phys. **84**, 5928 (1998).

[14]M. A. Lieberman, J. P. Booth, P. Chabert, J. M. Rax, and M. M. Turner, Plasma Sources Sci. Technol. **11**, 283 (2002).

[15]A. Perret, J. P. Booth, P. Chabert, J. Jolly, J. Guillon, and Ph. Auvray, Appl. Phys. Lett. **83**, 243 (2003).

[16]A. R. Ellingboe, U.S. patent 7,342,361 (11 March 2008).

[17]A. R. Ellingboe, D. O'Farrell, C. Gaman, F. Green, N. O'Hara, and T. Michna, *62nd Gaseous Electronic Conference*, Saratoga Springs, NY (2009).

[18]K. Ryan and A. R. Ellingboe, *37th European Physical Society Conference on Plasma Physics*, Dublin, Ireland (2010).

[19]E. Monaghan *et al.*, Thin Solid Films **519**, 6884 (2011).

[20]P. Chabert and N. Braithwaite, *Physics of Radio-Frequency Plasmas* (Cambridge University, Cambridge, 2011).

[21]T. Okumura, Phys. Res. Int. **2010**, 164249.

[22]K. N. Kim, J. H. Lim, G. Y. Yeom, S. H. Lee, and J. K. Lee, Appl. Phys. Lett. **89**, 251501 (2006).

[23]A. Mishra, K. N. Kim, T. H. Kim, and G. Y. Yeom, Plasma Sources Sci. Technol. **21**, 035018 (2012).

[24]T. H. Kim, K. N. Kim, A. Mishra, J. S. Seo, H. B. Jeong, J. O. Bae, and G. Y. Yeom, Jpn. J. Appl. Phys., Part 1 **52**, 05EA02 (2013).

[25]A. Mishra, T. H. Kim, K. N. Kim, and G. Y. Yeom, Plasma Sources Sci. Technol. **22**, 015022 (2013).

[26]A. Mishra, T. H. Kim, K. N. Kim, and G. Y. Yeom, J. Phys. D: Appl. Phys. **45**, 475201 (2012).

[27]S. Banna, A. Agarwal, G. Cunge, M. Darnon, E. Pargon, and O. Joubert, J. Vac. Sci. Technol., A **30**, 040801 (2012).

[28]D. J. Economou, J. Phys. D: Appl. Phys. **47**, 303001 (2014).

[29]S. Ashida, M. R. Shim, and M. A. Lieberman, J. Vac. Sci. Technol., A **14**, 391 (1996).

[30]S. Samukawa and S. Furuoya, Appl. Phys. Lett. **63**, 2044 (1993).

[31]A. Mishra, J. S. Seo, K. N. Kim, and G. Y. Yeom, J. Phys. D: Appl. Phys. **46**, 235203 (2013).

[32]A. Mishra, S. Lee, and G. Y. Yeom, J. Vac. Sci. Technol., A **32**, 061303 (2014).

[33]J. S. Seo, K. N. Kim, K. S. Kim, T. H. Kim, and G. Y. Yeom, Jpn. J. Appl. Phys., Part 1 **54**, 01AA10 (2015).

[34]S. K. Karkari, A. R. Ellingboe, C. Gaman, I. Swindells, and J. W. Bradley, J. Appl. Phys. **102**, 063308 (2007).

[35]S. K. Karkari, C. Gaman, A. R. Ellingboe, I. Swindells, and J. W. Bradley, Meas. Sci. Technol. **18**, 2649 (2007).

[36]R. B. Piejak, V. A. Godyak, R. Garner, B. M. Alexandrovich, and N. Sternberg, J. Appl. Phys. **95**, 3785 (2004).

[37]G. A. Curley, L. Gatilova, S. Guilet, S. Bouchoule, G. S. Gogna, N. Sirse, S. K. Karkari, and J. P. Booth, J. Vac. Sci. Technol., A **28**, 360 (2010).

[38]S. K. Karkari, A. R. Ellingboe, and C. Gaman, Appl. Phys. Lett. **93**, 071501 (2008).

[39]N. Sirse, M. H. Jeon, G. Y. Yeom, and A. R. Ellingboe, Plasma Sources Sci. Technol. **23**, 065046 (2014).

[40]M. V. Malyshev and V. M. Donnelly, Plasma Sources Sci. Technol. **9**, 353 (2000).

[41]M. A. Lieberman and S. Ashida, Plasma Sources Sci. Technol. **5**, 145 (1996).

[42]C. Gaman, Ph.D. thesis (Dublin City University, Ireland, 2011).

[43]J. Liu, Y. X. Liu, Z. H. Bi, F. Gao, and Y. N. Wang, J. Appl. Phys. **115**, 013301 (2014).

[44]N. Sirse, J. P. Booth, P. Chabert, A. Surzhykov, and P. Indelicato, J. Phys. D: Appl. Phys. **46**, 295203 (2013).

[45]S. Kim, M. A. Lieberman, A. J. Lichtenberg, and J. T. Gundmundsson, J. Vac. Sci. Technol., A **24**, 2025 (2006).

[46]A. Kono and K. Kato, Appl. Phys. Lett. **77**, 495 (2000).

[47]M. Shindo, Y. Ueda, S. Kawakami, N. Ishii, and Y. Kawai, Vacuum **59**, 708 (2000).

[48]G. A. Hebner and I. Abraham, J. Appl. Phys. **90**, 4929 (2001).

[49]N. Sirse, J. P. Booth, Y. Azamoum, and P. Chabert, *30th International Conference on Phenomena in Ionized Gases (ICPIG)*, UK (2011), pp. D13–292, available at http://mpserver.pst.qub.ac.uk/sites/icpig2011/292_D13_Sirse.pdf.

[50]G. Curley, Ph.D. thesis (Ecole Polytechnique, France, 2008).

[51]M. A. Lieberman and A. J. Lichtenberg, *Principles of Plasma Discharges and Materials Processing* (Wiley, New York, 1994).

[52]A. V. Vasenkov, X. Li, G. S. Oehrlein, and M. J. Kushner, J. Vac. Sci. Technol., A **22**, 511 (2004).

[53]M. Shimada, G. R. Tynan, and R. Cattolica, Plasma Sources Sci. Technol. **16**, 193 (2007).

[54]N. Sirse, Q. Delivre, J. P. Booth, and P. Chabert, *IEEE International Conference on Plasma Science* (ICOPS) (2012), p. 3P–135, available at http://ieeexplore.ieee.org/xpls/abs_all.jsp?arnumber=6383920&tag=1.

[55]G. A. Hebner and C. B. Fleddermann, J. Appl. Phys. **82**, 2814 (1997).

[56]A. Agarwal, P. J. Stout, S. Banna, S. Rauf, K. Tokashiki, J. Y. Lee, and K. Collins, J. Appl. Phys. **106**, 103305 (2009).